

THERMAL PERFORMANCE OF MULTI PIEZOELECTRIC FAN FOR ELECTRONIC COOLING APPLICATION USING 3-D DYNAMIC MESH

MUHAMMAD KHALIL ABDULLAH @ HARUN

UNIVERSITI SAINS MALAYSIA

2012

THERMAL PERFORMANCE OF MULTI
PIEZOELECTRIC FAN FOR ELECTRONIC
COOLING APPLICATION USING 3-D DYNAMIC
MESH

by

MUHAMMAD KHALIL ABDULLAH @ HARUN

Thesis submitted in fulfilment of the requirements for
the degree of
Doctor of Philosophy

JULY 2012

ACKNOWLEDGEMENTS

“In the name of ALLAH, The Most Beneficent, The Most Merciful”

Praise is exclusively to Allah. The Lord of the universe and Peace is upon the Master of the Messengers, his family and companions.

First of all, I would like to express deepest appreciations to my lovely parents; Rahmah and al-marhum Abdullah, and my siblings for their *doa* and continuous support throughout my life. Not to forget my lovely wife, Hadzirah and her family for their understanding and patience. Their continuous support enabled me fully concentrate this study.

I express my special thanks and heartfelt gratitude to my supervisor Prof. Mohd Zulkifly Abdullah and co-supervisor Assoc. Prof. Dr. Kamarul Arifin Ahmad for their patience, guidance, encouragement, support and valuable information on the electronic cooling, during my research. Not to forget Prof. Abdul Mujeebu, Akhi M. Zubair, Assoc. Prof. Zulkifli Mohamad Ariff for their guidance, opinion and suggestions.

My special thanks are also due to the Dean, Assoc. Prof. Dr. Zaidi Mohd Ripin and my colleagues in the vibration, control and instrumentation lab: W. Amri and M. Hashim for their contributions in the fabrication of the test apparatus and in the conduct of the noise and vibration experiments, and for help in conducting the control and instrumentation experiment. I also thank Dr. Erwan, Assoc. Prof. Dr. Shahrul Kamaruddin and Mr. Mohzani Mokhtar for the design optimization, and all

the staff of School of Mechanical Engineering, Universiti Sains Malaysia (USM) for their valuable supports and ideas on my research work.

My special thanks are also to the Electronic Cooling (Nazmi, Sufian, Mohamed, Tony, Lau and Sofwan), Electronic Packaging (Khor, Pak Dadan, Leong and Mior), Aerodynamic (Fauzi-aero, Hamid, Fairus and Fa-aero), Vibration and Fluid Structure Interaction (Najib, Tan, Gbum and Paklah), Optimization (Basher and Husaini) and Combustion (Kamal and Shahril) groups, who gave me inspiration to work hard and motivated me during thick and thin situations. I gratefully appreciate USM for its financial support on Fellowship Scheme and grants (1001/PMEKANIK/811076 and W-31-109-Eng-38). Last but not the least, my sincere thanks are to those who helped and supported me in one way or another.

Muhammad Khalil Bin Abdullah @ Harun

July 2012

TABLE OF CONTENTS

| | PAGE |
|--|-------------|
| ACKNOWLEDGEMENTS | ii |
| TABLE OF CONTENTS | iv |
| LIST OF TABLES | viii |
| LIST OF FIGURES | ix |
| NOMENCLATURES | xv |
| LIST OF ABBREVIATION | xix |
| ABSTRAK | xxi |
| ABSTRACT | xxiv |
| CHAPTER 1: INTRODUCTION | |
| 1.0 Overview | 1 |
| 1.1 Introduction | 1 |
| 1.2 Problem Statement | 4 |
| 1.3 Objective of the Research | 5 |
| 1.4 Scope of the Research Work | 6 |
| 1.5 Thesis Outline | 7 |
| CHAPTER 2: LITERATURE REVIEW | |
| 2.0 Overview | 8 |
| 2.1 Cooling of Microelectronics Device | 8 |
| 2.2 Experiments on Piezofan in Fluidic Studies | 11 |
| 2.2.1 Single-fan Oscillation | 11 |
| 2.2.2 Multi-fan Oscillation | 15 |
| 2.3 Experiments on Piezofan in Heat Transfer | 18 |
| 2.3.1 Single-Fan Configuration | 18 |

| | | |
|-------------------------------|---|----|
| 2.3.2 | Multi-fan Configuration | 20 |
| 2.4 | Numerical Studies on the Movement Object in Fluid | 21 |
| 2.4.1 | Acoustic Streaming Flow | 21 |
| 2.4.2 | Discrete Vortex Method (DVM) | 24 |
| 2.4.2 | Arbitrary Lagrangian Eulerian (ALE)/Dynamic Mesh | 25 |
| 2.5 | Optimization of the Piezofan | 33 |
| 2.6 | Application of Piezofan in Electronic Cooling | 36 |
| 2.7 | Concluding Remarks | 38 |
| CHAPTER 3: METHODOLOGY | | |
| 3.0 | Overview | 40 |
| 3.1 | Introduction to the Numerical Method | 40 |
| 3.1.1 | Governing Equations | 41 |
| 3.1.2 | Turbulence Model | 44 |
| 3.1.2.1 | Two-equation Turbulence Model | 45 |
| 3.1.2.2 | Near-wall Treatment | 46 |
| 3.2 | Prescribed of Dynamic Mesh and Mesh Updates | 50 |
| 3.3 | Dynamic Zones and Parameters Setup | 51 |
| 3.3.1 | Spring-Based Smoothing Method | 51 |
| 3.3.2 | Remeshing Method | 53 |
| 3.4 | Numerical Schemes | 54 |
| 3.5 | Computational Model | 55 |
| 3.6 | Grid System | 57 |
| 3.7 | Beam (Piezofan) Deflection Model | 60 |
| 3.8 | Compiling Special Command using User-Defined Function (UDF) | 64 |
| 3.9 | Computational Model Setup | 65 |

| | | |
|--|---|-----|
| 3.10 | Simulation Procedure | 67 |
| 3.11 | Model Validation | 69 |
| 3.12 | Time-step and Grid Dependency Analysis | 71 |
| 3.13 | Experimental Set-up | 79 |
| 3.13.1 | Vibration Characteristics | 79 |
| 3.13.2 | Flow Visualization | 83 |
| 3.13.3 | Thermal Performance | 86 |
| 3.14 | Experimental procedure | 91 |
| 3.15 | Design of Experiment (DOE) | 92 |
| 3.16 | Summary | 96 |
| CHAPTER 4: RESULTS AND DISCUSSION | | |
| 4.0 | Overview | 97 |
| 4.1 | Vibration Characteristics of the Piezofan | 97 |
| 4.2 | Flow Visualization in the Miniature System | 99 |
| 4.3 | Numerical Studies of Single-fan | 104 |
| 4.4 | Flow Characteristic Studies of Multi-fan | 117 |
| 4.5 | Comparison of Single-fan and Multi-fan Flow Characteristics | 121 |
| 4.6 | Heat Transfer Study of Piezofan | 131 |
| 4.6.1 | Single-fan Heat Transfer Characteristics | 131 |
| 4.6.2 | Multi-fan Heat Transfer Characteristics | 134 |
| 4.6.3 | Comparison of Single-fan and Multi-fan Heat Transfer Characteristics | 136 |
| 4.7 | Numerical Studies on the Effect of Piezofan Orientation | 147 |
| 4.8 | Multi-fan with Various Configurations of Heat Sink | 153 |
| 4.9 | Optimization of Multi-fan Configuration Using DOE | 160 |

| | | |
|---|---|-----|
| 4.9.1 | Analysis of Variance (ANOVA) | 161 |
| 4.9.2 | Effectiveness of Temperature Drop | 166 |
| 4.10 | Numerical Study on the Effect of Tip Gap (δ) on Temperature Drop | 174 |
| 4.11 | Numerical and Experimental Study on the Effect of Reynolds Number | 180 |
| 4.12 | Comparison against Traditional Heat Removal Techniques | 192 |
| CHAPTER 5: CONCLUSIONS AND FUTURE WORK | | |
| 5.0 | Conclusions | 197 |
| 5.1 | Preliminary Investigations | 197 |
| 5.2 | Parametric studies on Multi Piezofan | 199 |
| 5.3 | Applicability study | 202 |
| 5.4 | Recommendation and Suggestions for Future Work | 203 |
| REFERENCES | | 204 |
| LIST OF PUBLICATIONS | | 214 |
| APENDICES | | |
| | Appendix A: MATLAB Programming | 215 |
| | Appendix B: UDF File-Sinusoidal Input | 216 |

LIST OF TABLES

| | PAGE |
|---|-------------|
| 2.1 Thermal solutions for electronics cooling. | 10 |
| 3.1 Piezofan properties. | 60 |
| 3.2 Time step size with specified symbols | 72 |
| 3.3 Various mesh size with specified symbols. | 75 |
| 3.4 Comparison of experimental and simulation temperatures for grid independency study. | 79 |
| 3.5 Specifications of the piezofan. | 82 |
| 3.6 Values for the parameters investigated. | 92 |
| 3.7 Independent variables of the CCD design. | 94 |
| 4.1 Single-fan and multi-fan comparison of experimental and simulation temperatures. | 139 |
| 4.2 Comparison of temperature for heater and heat sink. | 160 |
| 4.3 ANOVA results for significant model terms. | 163 |
| 4.4 ANOVA results for response surface quadratic model. | 164 |
| 4.5 Optimization results for maximum temperature drop | 170 |
| 4.6 Comparison of experimental and simulation temperatures for different configuration. | 172 |

LIST OF FIGURES

| | PAGE |
|---|-------------|
| 2.1 Side and front views of oscillating plates and experimental arrangement (Ihara and Watanabe, 1994) | 16 |
| 2.2 Schematic of different experimental configurations (Acikalin et al., 2007) | 36 |
| 2.3 Piezofan used in the portable products cooling experiment (Acikalin et al., 2004) | 37 |
| 3.1 Subdivisions of near-wall region (Salim and Cheah, 2009). | 47 |
| 3.2 Wall Treatments (FLUENT, 2006). | 49 |
| 3.3 Dynamic mesh smoothing command | 52 |
| 3.4 Dynamic mesh remeshing command | 53 |
| 3.5 Visualization of discrete cells. | 55 |
| 3.6 Illustration of the boundary conditions | 56 |
| 3.7 Combination of tetrahedral and quad literal elements. | 58 |
| 3.8 Separated boundary domains. | 59 |
| 3.9 Grid interface command. | 60 |
| 3.10 Piezofan locations with respect to time at different A/G | 62 |
| 3.11 Beam velocities at different positions of beam | 63 |
| 3.12 C compiled command. | 64 |
| 3.13 Steps in CFD analysis. | 68 |
| 3.14 Contours of the heat transfer coefficient (a) on the heated surface in the experiment of Kimber et al. (2007) and (b) on the uniform heat flux surface in the three dimensional model. | 70 |
| 3.15 Comparison of predicted and experimentally determined heat transfer coefficient, h (Kimber et al. 20007). | 71 |
| 3.16 Time step solutions of the beam. | 73 |

| | | |
|------|--|-----|
| 3.17 | (a) Temperature measuring positions and (b) its variation over time. | 74 |
| 3.18 | Comparison between the temperature field obtained by (a) coarse, (b) FM-I and (c) FM-II. | 75 |
| 3.19 | Reference line for temperature (a) x -direction and (b) z -direction. | 76 |
| 3.20 | Simulation temperature distributions along the fin (a) x -direction and (b) z -direction of the flat plate. | 77 |
| 3.21 | Velocity gradients at the wall between CM and FM. | 78 |
| 3.22 | (a) Schematic and (b) photographs of the experimental setup to study the vibration parameters | 80 |
| 3.23 | Schematic diagram of the piezofan beam and inverter drive circuit | 82 |
| 3.24 | Variation of power as a function of voltage | 83 |
| 3.25 | (a) Schematic and (b) photographs of the experimental set-up for flow visualization | 84 |
| 3.26 | (a) Schematic and (b) photographs of the experimental setup for heat transfer | 87 |
| 3.27 | Schematic of different experimental configurations (all dimension in mm and not in scale) | 88 |
| 3.28 | Schematic diagram of fans (a) pitch (all dimension in mm) (b) α , δ , tip gap and height for the fan and (c) photograph of a sample in heat transfer experiments | 89 |
| 3.29 | Thermocouples location in different configurations | 90 |
| 4.1 | Vibration amplitude and frequency behaviour of the piezofan. | 98 |
| 4.2 | Effect of electric field to the piezofan amplitude. | 99 |
| 4.3 | Experimental vectors plot for $\delta = 0.1$, when piezofan swings (a) right and (b) left. | 101 |
| 4.4 | Simulation vector plot for $\delta = 0.1$ at different piezofan positions. | 101 |

| | | |
|------|---|-----|
| 4.5 | Experimental vectors plot for $\delta = 0.17$, when piezofan swings (a) right and (b) left. | 103 |
| 4.6 | Simulation vector plot for $\delta = 0.1$ at different piezofan positions. | 103 |
| 4.7 | Comparison of the computed maximum velocity with the experimental flow visualization for given time instant. | 103 |
| 4.8 | Vortex formation at different swinging positions of the piezofan (for $\delta = 0.17$) | 104 |
| 4.9 | Schematic diagrams representing vibrating piezofan at different phase intervals. | 106 |
| 4.10 | Velocity vectors at different phase intervals. | 108 |
| 4.11 | Pressure distributions and streamlines at different phase intervals. | 110 |
| 4.12 | Path line released at different phase intervals. | 112 |
| 4.13 | Side and top views of path line released. | 115 |
| 4.14 | Mean velocity profiles over a period of the piezofan deflection along (a) x -direction and (b) z -direction. | 116 |
| 4.15 | Velocity vectors at different phase intervals produced by the multi-fan. | 118 |
| 4.16 | Mean velocity profiles over a period of the piezofan deflection along (a) x -direction and (b) z -direction for multi-fan. | 120 |
| 4.17 | Comparison of velocity vectors of single-fan and multi-fan at different phase intervals. | 122 |
| 4.18 | Comparison of mean velocity distribution downstream of piezofan. | 125 |
| 4.19 | Comparison of pressure distributions and streamlines single-fan and multi-fan at different phase intervals. | 128 |
| 4.20 | Vorticity magnitudes and streamlines for single-fan and multi-fan during 50 periods. At this instant the piezofan is passing its original position. | 130 |
| 4.21 | Experimental temperature variations for the single-fan. | 132 |

| | | |
|------|--|-----|
| 4.22 | Temperature distribution along x -direction due to single-fan jet velocity at (a) $G/A = 0.1$ and (b) $G/A = 1$ during 50 periods from simulation. | 133 |
| 4.23 | Temperature variations for the multi-fan. | 134 |
| 4.24 | Temperature distribution along x -direction due to multi-fan jet velocity at (a) $G/A = 0.1$ and (b) $G/A = 1$ during 50 periods from simulation. | 135 |
| 4.25 | Temperature drop for single-fan and multi-fan at $\alpha = 90^\circ$ and $\delta = 0.17$ (S = single-fan and M = multi-fan). | 137 |
| 4.26 | Temperature contours of flat plate during natural convection. | 138 |
| 4.27 | Comparison of temperature contours and labels between (a) single-fan and (b) multi-fan during 50 periods. | 139 |
| 4.28 | Heat transfer coefficients from three different experiments along with the natural convection value (S = single-fan and M = multi-fan). | 142 |
| 4.29 | Heat transfer coefficient plots along the (a) x -direction and (b) z -direction of the flat plate during natural convection. | 143 |
| 4.30 | Heat transfer coefficient plots along the (a) x -direction and (b) z -direction of the flat plate for two different fans configurations during 50 periods. | 145 |
| 4.31 | Comparison of velocity and temperature profiles between single-fan and multi-fan. | 147 |
| 4.32 | Comparison of temperature contours in term of angle orientation at $\delta = 0.17$ during 50 periods. | 149 |
| 4.33 | Heat transfer coefficient plots along the x -direction of the flat plate for different piezofan orientation during 50 periods. | 150 |
| 4.34 | Heat transfer coefficients from three different orientations along with the natural convection value. | 152 |
| 4.35 | Velocity and temperature profile on different piezofan orientation. | 153 |
| 4.36 | Temperature variations for the configurations. | 154 |
| 4.37 | Comparison of temperature drops in the configurations. | 156 |

| | | |
|------|--|-----|
| 4.38 | Comparison of three configurations (A, B and C), illustrating the effect of inclusion of the fin. | 157 |
| 4.39 | Natural convection of configuration C. (a) Simulation and IR camera images (b) side, (b) top view. | 158 |
| 4.40 | Force convection of configuration C. (a) Simulation and IR camera images (b) side, (b) top view. | 159 |
| 4.41 | Normal probability plots of the studentized residuals. | 165 |
| 4.42 | Comparison of actual and predicted temperature drop. | 166 |
| 4.43 | 3D surface and contour plots for temperature drop as a function of α and δ . | 167 |
| 4.44 | Temperatures drop for the configurations. | 169 |
| 4.45 | Comparison of temperature contours on each configuration during 50 periods. | 171 |
| 4.46 | Heat transfer coefficient plots along the x -direction. | 173 |
| 4.47 | Heat transfer coefficients from different configurations along with the flat plate natural convection value. | 174 |
| 4.48 | Vorticity magnitudes and streamlines for (a) $\delta = 0.17$ and (b) $\delta = 0.03$ during 50 periods. | 175 |
| 4.49 | Temperature contours of configuration C during natural convection. | 176 |
| 4.50 | Comparison of temperature contours between (a) $\delta = 0.17$ and (b) $\delta = 0.03$ during 50 periods. | 178 |
| 4.51 | Velocity and temperature profile along x -horizontal direction at different δ . | 179 |
| 4.52 | Heat transfer coefficient plots along the x -direction of the flat plate for two different gaps. | 180 |
| 4.53 | Comparison of temperature contours and labels on configuration C for different Re during 50 periods. | 182 |
| 4.54 | Velocity and temperature profile along x -horizontal direction at different Reynolds number. | 184 |
| 4.55 | Heat transfer coefficient plots along the (a) x -direction and (b) z -direction of the configuration C for different Re. | 186 |

| | | |
|------|--|-----|
| 4.56 | Heat transfer coefficients from different Reynolds number along with the natural convection value. | 187 |
| 4.57 | Comparison of local heat transfer coefficient between simulation and experiment. | 188 |
| 4.58 | Comparison of predicted and experimentally determined local Nusselt number. | 191 |
| 4.59 | Prediction of an average Nusselt number. | 191 |
| 4.60 | Two commercial rotary fans. | 193 |
| 4.61 | Comparison of power and noise consumption against rotational fans. | 195 |
| 4.62 | Comparison of power and volume ratios against rotational fans. | 196 |

NOMENCLATURES

| SYMBOL | DESCRIPTION | UNIT |
|------------------------|--|-----------|
| English Symbols | | |
| A | Frequency dependent amplitude | m^2 |
| A_f | Movement area (FLUENT) | - |
| C | Correlation constant | - |
| C_f | Coefficient of skin friction | - |
| d | Correlation power constant | - |
| D | Cross-diffusion term | - |
| D_{pz} | Hydraulic diameter of vibration envelope | m |
| E | Total energy | W |
| e | Fluids internal energy | W |
| e_i | error | - |
| F | Fisher variation ratio | - |
| G | Gap between piezofan and heat sink | m |
| \tilde{G}_k | Generation of turbulence kinetic energy | - |
| \tilde{G}_ω | Generation of ω | - |
| g | Gravitational acceleration | m/s^2 |
| h | Sensible enthalpy | j/kg |
| h_{fin} | Fin height | m |
| h_{local} | Local heat transfer convection coefficient | W/m^2K |
| h_{avg} | Average heat transfer convection coefficient | W/m^2K |
| J_j | Diffusion flux of species | - |
| k | Turbulent kinetic energy | m^2/s^2 |
| k_a | Thermal conductivity of air | W/mK |

| | | |
|-------------------|------------------------------------|------------------|
| k_{doe} | Number of factors | - |
| k_{eff} | Effective thermal conductivity | W/mK |
| k_f | Fluid thermal conductivity | W/mK |
| k_g | General thermal conductivity | W/mK |
| k_s | Solid thermal conductivity | W/mK |
| L | Total piezofan length | m |
| l_h | Length of heater | m |
| l_{hs} | Length of heat sink | m |
| l_p | Length of piezofan patch | m |
| l_u | Length of un-patch piezofan | m |
| Nu_{local} | Local Nusselt number | - |
| Nu_{avg} | Average Nusselt number | - |
| P | Static pressure | N/m ² |
| Q_{in} | Power input | W |
| q | Heat flux | W/m ² |
| \dot{q}_h | Heat generation | W/m ³ |
| R_b | Solid thermal resistant | K/W |
| R_{conv} | Fluid convection thermal resistant | K/W |
| R^2 | Correlation coefficient | - |
| S | Source term | - |
| SD | Standard deviation | - |
| T | Temperature | K |
| T_{base} | Average heat sink base temperature | K |
| T_j | Junction temperature | K |
| $T_{n=1,2,\dots}$ | Temperature at a n-point | K |

| | | |
|----------------------|---|----------------|
| T_h | Temperature of heater | K |
| T_{s-exp} | Experiment heat sink surface temperature | K |
| T_{s-sim} | Simulation heat sink surface temperature | K |
| T_∞ | Ambient temperature | K |
| \bar{T} | Dimensionless temperature | - |
| t | Time | s |
| t_{ep} | Epoxy thickness | m |
| t_h | Heater thickness | m |
| t_{hs} | Heatsink thickness | m |
| \vec{u} | Velocity vector | m/s |
| u_g | Grid velocity | m/s |
| V | Control volume | m ³ |
| V_{rms} | Root mean square of the velocity of fan tip | m/s |
| \vec{v} | Velocity vector | - |
| w | Blade position | m |
| \dot{w} | Blade velocity | m/s |
| w_h | Heater width | m |
| w_p | Width of piezofan | m |
| x, y, z | Space coordinates | m |
| X | Variable value | - |
| Y | Dissipation coefficient | - |
| Y_r | Response value | - |
| Greek Symbols | | |
| α | Angle | ° |
| β | Eigen value | - |

| | | |
|---------------|---------------------------------------|-------------------|
| β_0 | Constant coefficient | - |
| β_j | Linear interaction coefficient | - |
| β_{jj} | Quadratic interaction coefficient | - |
| β_{ij} | Second-order terms | - |
| δ | Normalized tip gap | - |
| ρ | Fluid density | kg/m ³ |
| τ | Viscous stress tensor | Pa |
| τ_w | Wall shear stress | Pa |
| Γ | Diffusion coefficient | - |
| Φ | General scalar for transport equation | - |
| ν | Kinematic viscosity of air | m ² /s |
| ω | Ratio of ε to k | - |
| ω_b | Beam angular velocity | rad/s |
| ω_f | Free stream values | - |
| ω_{vf} | Vibration frequency | 1/s |

LIST OF ABBREVIATION

| | |
|------------|-----------------------------------|
| 2-D | Two-dimensional |
| 3-D | Three-dimensional |
| AC | Alternate current |
| ALE | Arbitrary Lagrangian-Eulerian |
| ANOVA | Analysis of variance |
| BSL | Baseline |
| CCD camera | Charge-coupled device |
| CCD | Central Composite Design |
| CFD | Computational fluid dynamics |
| CM | Coarse mesh |
| Conf. | Configuration |
| COP | Coefficient of performance |
| DAQ | Data acquisition systems |
| DC | Direct current |
| DOE | Design of experiment |
| DVM | Discrete vortex method |
| EMCF | Electromechanical coupling factor |
| ESA | Evolution Strategy Algorithm |
| FE | Finite element |
| FM | Fine mesh |
| FSI | Fluid structure interaction |
| FVM | Finite volume method |
| GCL | Geometric Conservation Law |

| | |
|-----------------------|--|
| IC | Integrated circuit |
| LED | Light emitting Diode |
| LES | Large eddy simulation |
| LSI | Large scale integration |
| Nu_{local} | Local Nusselt number |
| Nu_{avg} | Average Nusselt number |
| OFAT | One experimental/simulation factor at a time |
| PC | Personal computer |
| PIV | Particle image velocimetry |
| PVDF/PVF ₂ | Polyvinylidene Flouride |
| PZT | Lead zirconate titanate |
| RANS | Reynolds average Navier Stokes |
| Re | Reynolds number |
| RS | Response surface |
| RSM | Response surface methodology |
| SBVG | Sub-boundary layer vortex generator |
| SD | Standard deviation |
| SIMPLE | Semi-implicit pressure-linked equations |
| SST | Shear stress transport |
| TIM | Thermal interface materials |
| TS | Time step |
| UDF | User defined function |
| VAC | Voltage alternating current |

**PRESTASI TERMA BAGI KIPAS PIEZOELEKTRIK BERBILANG UNTUK
APLIKASI PENYEJUKAN ELEKTRONIK DENGAN JARINGAN
DINAMIK 3-D**

ABSTRAK

Kipas piezoelektrik (selepas ini dinamakan sebagai kipas piezo) boleh dimanipulasikan untuk menjana aliran udara bagi penyejukan peranti mikroelektronik. Ia mempamerkan ciri-ciri cemerlang seperti bebas-bunyi ketika beroperasi, penggunaan kuasa yang rendah dan sesuai digunakan pada ruang yang sempit. Tujuan utama kajian ini adalah untuk menyiasat prestasi aliran dan haba kesian daripada ayunan piezofan melalui penggunaan pemodelan berangka. Perisian komersial CFD FLUENT 6.3.2TM digunakan untuk menyelesaikan persamaan-persamaan Purata Reynolds Navier Stokes (RANS) dengan mempertimbangkan model pengangkutan tegasan ricih (SST) $k-\omega$. Gerakan harmonik mod pertama dalam rasuk ubah bentuk (piezofan) dibangunkan dengan menggunakan bahasa C, dan ditetapkan di bawah opsyen jaringan dinamik dengan bantuan fungsi tetapan pengguna (UDF). Struktur jaringan hibrid telah digunakan iaitu; jaringan tetrahedron telah bekerja sekitar pesongan piezofan dalam usaha untuk mengelakkan jumlah sel negatif, manakala untuk kawasan yang selebihnya, jaringan prisma telah digunakan untuk mendapat hasil ketepatan yang lebih baik. Satu teknik jaringan bergerak berasaskan spring iaitu kaedah pelicinan dan bersirat telah digunakan untuk membolehkan ayunan sempadan kipas piezo. Keputusan kajian simulasi telah menunjukkan keserasian yang baik dengan ukuran velocimetri imej zarah (PIV). Kejayaan pendekatan ini kemudian digunakan ke dalam bidang aliran dan

pemindahan haba pada ayunan kipas-tunggals dan kipas-berbilang ke atas plat rata (kecerunan tekanan sifar) dengan mengambil kira kesan dinding; kesan y^+ ($y^+ \approx 1$) pada jurang yang telah ditetapkan iaitu δ (nisbah ketinggian jurang ke ketinggian sirip). Kajian juga telah dijalankan terhadap kesan sudut orientasi (α) di mana ia menunjukkan bahawa kipas-berbilang dan pada orientasi sudut normal mempunyai pengaruh yang besar ke atas prestasi pemindahan haba. Seterusnya, satu kajian parametrik telah dilakukan untuk memaksimumkan prestasi haba di mana sudut orientasi (α), sela jarak hujung (δ) dan konfigurasi beberapa sink haba (A, B dan C), dengan menggunakan pendekatan pengoptimuman Rekabentuk Eksperimen (DOE). Daripada 13 percubaan eksperimen yang ditentukan oleh Rekabentuk Komposit Berpusat (CCD), didapati α , δ dan konfigurasi terbaik pada sudut 90° , sela jarak hujung 0,17 dan konfigurasi dengan empat sirip (C). Selepas itu, kajian selanjutnya telah dilakukan dengan menetapkan α pada 90° dan konfigurasi C digunakan, δ pula telah dipendekkan kepada 0.03 dan nombor Reynolds divariasikan daripada 930 kepada 2460. Antara parameter-paramter yang diuji berikutnya, orientasi normal dengan minimum jurang hujung ($\delta = 0.03$) didapati memberi prestasi yang terbaik apabila dikendalikan dengan amplitud ayunan tertinggi (maksimum nombor Reynolds). Pada kedudukan ini, pekali pemindahan haba meningkat kepada 130%, berbanding dengan kes itu tanpa piezofan. Keputusan berangka kemudiannya dibandingkan dengan penemuan uji kaji dan didapati berada dalam keserasian yang baik. Satu kajian kebolehpakaian telah dibuat antara penyejukan hibrid kipas-berbilang dengan penyelesaian penyejukan hibrid konvensional iaitu kipas berputar dari segi hingar, nisbah kuasa dan isipapadu gunaan pada prestasi penyejukan yang sama. Kajian telah mendapati bahawa tahap hingar, nisbah kuasa dan isipadu gunaan

yang dihasilkan oleh kipas-berbilang lebih kecil berbanding penyelesaian konvensional.

THERMAL PERFORMANCE OF MULTI PIEZOELECTRIC FAN FOR ELECTRONIC COOLING APPLICATION USING 3-D DYNAMIC MESH

ABSTRACT

Piezoelectric fan (hereafter name as piezofan) can be manipulated to generate airflow for cooling microelectronic devices. Its outstanding features include noise-free operation, low power consumption and suitability for confined spaces. The main aim of the present study was to investigate the performance of an oscillating piezofan through the use of numerical modeling. The commercial CFD software Fluent 6.3.2TM was used to solve the Reynolds Averaged Navier Stokes (RANS) equations with the consideration of shear stress transport (SST) $k-\omega$ model. The harmonic motion of the first mode in the deforming beam (piezofan) was developed using C language, and was set under dynamic mesh option with the help of a user defined function (UDF). A hybrid mesh was employed, with tetrahedral mesh used around the piezofan deflection region in order to avoid negative cell volumes, and a structured, prism mesh in the remaining envelop. The spring-based smoothing and remeshing methods were employed to allow for oscillation of the piezofan boundaries. The results revealed good agreement with the limited particle image velocimetry (PIV) measurements available. This successful approach was then employed in the study of flow field and heat transfer for both single-fan and multi-fan oscillation over flat plate with consideration of wall effect i.e. y^+ effect ($y^+ \approx 1$) at a fixed tip gap of δ (the ratio of gap height to fin height). Study carried on the effect of orientation angle (α) showed that the multi-fan and normal orientation had significant influence on the performance of heat transfer. A parametric study was

carried out in order to maximize the heat removal ability by considering parameters such as orientation angle, and tip gap spacing (δ) in several configurations of heat sink, using the popular Design of Experiments (DOE) approach. Out of the 13 experimental trials determined by Central Composite Design (CCD), the best α , δ and configuration were found to be 90° , 0.17 and configuration with four fins respectively. Subsequent tests were carried out keeping α as 90° and configuration C, δ being decreased to 0.03 and the Reynolds number varied from 930 to 2460. The results showed that the normal orientation with the minimum tip gap ($\delta = 0.03$) was found to give the best performance when operated with the highest amplitude of oscillation (maximum Reynolds number). At this setting, the heat transfer coefficient increased to 130%, when compared to the case without piezofans. The numerical result was then compared with the experimental findings and was found to be in good agreement with each other. An applicability study between hybrid cooling multi-fan and the conventional hybrid cooling solution i.e. rotary fan in terms of noise level, power and volume ratios at the same cooling performance was also accomplished. It was found that the noise level, power and volume ratios produced by the multi-fan was significantly lesser compared to those conventional solutions.

CHAPTER 1

INTRODUCTION

1.0 Overview

An introduction to the thermal management of microelectronic devices was presented in this chapter. The importance of thermal management for electronic applications, significance of piezoelectric fan in heat transfer and its commercial viability were discussed. The remainder of the section explained the problem statement, objectives and scope of the present study, followed by the outline of the thesis.

1.1 Introduction

Thermal management has been an essential requirement for the rapid growth of electronic industry. As the circuit density and power dissipation of integrated circuit (IC) chips were increasing, the associated heat flux levels become crucial. The large amount of heat flux could create unusual heat stress on chips, substrate, and its package. The performance of the electronic devices was directly related to the temperature; therefore it was important to maintain them within the acceptable temperature levels. Decreasing the temperature of a component increased its performance as well as its reliability (Ohadi and Qi, 2005).

Natural convection cooling was obviously advantageous for low power dissipating devices since it offered low-cost, energy-free, and noise-free operation (Tou et al., 1999; Adam et al., 1999). An additional means of passive cooling namely heat sink has been adapted to natural convection, for maintaining the

operating temperature of electronic components at a satisfactory level (Ledezma and Bejan, 1995). The most common method for cooling electronic devices was to use finned heat sinks usually made of aluminum; it provided a large surface area for the dissipation of heat and effectively reduced the thermal resistance (Ismail et al., 2008). Heat sinks were commonly attached to the surface of the spreader to provide additional surface area. Unfortunately, due to surface roughness the physical contact at the interface of the electronic component and the heat spreader was only around 5% of the total contact area (Bailey, 2008). This lack of contact could significantly limit the heat transfer from the component to the heat sink; however, the recently introduced thermal gap pad could increase the contact surface thereby reducing the contact resistance (Lee, 2010).

Nevertheless, the rising demand for high performance and multi functionality in electronic devices posed thermal challenges that may not be tackled by passive cooling techniques; this situation calls for active cooling techniques (Arularasan and Velraj, 2008). Combination of rotary fans and heat sinks has been a relatively feasible option, as it requires no special packaging considerations. On the other hand, even applications with lower heat dissipation levels could pose severe challenges due to space, weight, power consumption, noise level, or other constraints (Garimella, 2006); for instance, the more the heat generated the larger, faster and noisier was the fan needed to remove it. One of the techniques proposed over the last decade to cope up with this issue was piezoelectric fan (Toda and Osaka, 1979; Acikalin et al., 2003).

Piezoelectric fan (hereafter named as piezofan) was a cantilever blade whose vibration was actuated by means of a piezoelectric element and it was typically bonded near the clamped end of the blade. A bending moment was induced at the interface of the cantilever blade and the piezoelectric element when a voltage was applied (Kim et al., 2005; Wait et al., 2007). The blade was set into an oscillatory motion if an alternating voltage was applied. This produced oscillations throughout the blade, and as the actuation frequency was tuned to that of the fundamental resonance frequency of the piezofan, large-amplitude vibration occurred at the free end of the cantilever blade, serving to agitate and move the surrounding fluid. This piezofan have been shown to provide substantial enhancements in heat transfer when compared to natural convection alone (Acikalin et al., 2004).

Piezofan has received some attention for use in cooling applications throughout the last few decades. A number of advantages particular to piezofan have been addressed as an attractive thermal management solution. First, this piezofan consumed very little power typically operated in the range of 1-40 mW, making them ideal candidates for applications where power consumption was a key issue such as a cell phone, PDA, or other mobile device. Second; it could also be built to meet different geometric constraints for many applications, and can exploit any available volume envelope. Third; most of this device was driven at frequencies under 100 Hz so that the acoustic energy and noise levels were kept low such that their first mode of resonance was outside the range of frequencies audible to the human ear in order to ensure silent operation. Another advantage when compared to a traditional rotary fan, this device also had no moving parts, which ultimately led to longer life and better reliability.

1.2 Problem Statement

Previous researchers focused on feasibility and performance characteristics of a single-fan, while multi-fan, which had important practical applications, was not widely studied (Kimber et al., 2009a). Even though, multi-fan was introduced to enhance the fluid flow as well as heat transfer recently, they however focused their attention to cooling of heat source (Kimber et al., 2009b). No studies were carried out to verify the usefulness of multi-fan in conjunction with heat sink, which was more practical in electronic cooling applications.

Numerical modeling of objects in motion under fluid domain was a complicated study. It can be inferred from the previous works that dynamic mesh was used to evaluate the interaction between fluid phenomena due to deformation on account of motion (Zulkefli et al., 2010; Ahmad et al., 2011). Hybrid mesh was employed to overcome the negative volume effect. However, most of the studies on piezofan simulation primarily focused on 2-D dynamic mesh flow, and only few preliminary works were accomplished using 3-D dynamic mesh (Zaitsev et al., (2007). Moreover, it did not take into account the effect of heat transfer.

It was also observed that most studies employed laminar boundary regimes in order to simply their works in spite the fact that piezofan motion results in localized turbulent behavior and therefore has significant impact on the wall boundaries (Ahmad et al., 2008; 2011; Cengel, 2003). This requires flow modeling to consider turbulence models to resolve flow issues and also consider wall effect i.e. y^+ in the simulation either 2-D or 3-D. The oscillating piezofan was intrinsic to the oscillatory unsteady flow and among the relevant flow parameters involved were oscillation

orientation, tip gap distance and oscillation amplitude (Reynolds number). These were the parameters that had significant influence on the flow field and heat transfer. This was due to the oscillating piezofan over the heat sink surface embedded with turbulent boundary layer, which was also analogous to the thermal boundary layer effect.

Numerical and Experimental studies had certain limitations with respect to identifying the combination of best possible parameters that would enhance heat transfer. It demands several trials and permutations to achieve the best combination. However, by using DOE approach the optimization of heat transfer becomes simpler and helps optimize values of the parameters, even if actual experiments were not conducted with these values. The usefulness of these statistical tools which can predict accurate combinations can save a lot of experimental and simulation time and cost. Unfortunately this state of art tool has rarely been used in the study of piezo fan applications.

In general, there were several gaps in research with respect of use of piezofan application which needed serious attention even before initiating its commercial usage.

1.3 Objective of the Research

The aims of this research were threefold: Firstly, to simulate the interaction between flow and oscillating piezofan, and investigate the flow and heat transfer performance of an oscillating single-fan and multi-fan. This was accomplished using numerical solution of the Reynolds average Navier Stokes (RANS) equations considering wall

effects and validated with experimental findings. Secondly, several parametric studies were carried out to account for the best possible multi-fan set up that could establish better thermal performance. This also established the standardization of piezofan set up for best possible heat transfer characteristics. And a comparison was carried out between the proposed cooling solution (the best configuration), with the conventional hybrid cooling solution, in order to determine its effectiveness in terms of heat transfer. The aims included the following objectives:

- a. To conduct 3-D numerical investigation of single-fan and multi-fan and study their effects on flow and heat transfer.
- b. To carry out experimental studies and validate the numerical model developed.
- c. To study the flow interaction due to piezofan deflection and the turbulent boundary layer (wall effect).
- d. To investigate the effect of parameters involved in the flow and heat transfer interaction, such as heat sink design, temperature drop, mean velocity, heat transfer coefficient, and Reynolds and Nusselt number.
- e. To compare the standardized piezofan configuration with the conventional heat removal methods.

1.4 Scope of the Research

In this study, single-fan and multi-fan were investigated as a hybrid cooling technique for the thermal management of microelectronics. The experimental investigations were then illustrated by the numerical simulations. Three different types of heat sinks were studied. In the flat plate configuration, fin was excluded while in the rest; two and four fins were considered. In the two and four fins

configurations, the fins were extended in the entire length on the plate. The piezofans were fixed at the certain pitch, while kept at various tip gap and angles to the heat sink. Since large number of variables affected the heat transfer in this experiment, a design of experiments (DOE) approach was used to allow optimal values of the parameters to be predicted. The developed model was then compared with the conventional heat removal techniques to evaluate its performance characteristics.

1.5 Thesis Outline

This thesis was organized into five chapters. Chapter 1 dealt with introduction to thermal management and piezofan. In addition, problem statement, objectives and scope of research were also presented. In Chapter 2, the literature review wherein the modern cooling techniques available were explored and demonstrated the effectiveness of piezofan for microelectronic cooling. The methodology was presented in Chapters 3, where it had two segments. First segment described the numerical setup such as computational model, mesh generation, governing equation, turbulence model, prescribed mesh motion and mesh updates, blade displacement model, model setup and simulation procedure, and validation of the present approach. Second segment described the experimental setup and procedure and Design of Experiment (DOE). Results, discussion and analysis in term of thermal performance such as temperature drop, dimensionless temperature, heat transfer coefficient, effect of Reynolds and Nusselt numbers to the cooling mechanism, and comparison between conventional cooling were presented in Chapter 4. Finally, conclusion and recommendation for future works was discussed in Chapter 5.

CHAPTER 2

LITERATURE REVIEW

2.0 Overview

The purpose of this chapter is to provide a thorough review of the current and past works applicable to piezofan and its applications to electronic cooling. Initially a brief overview on cooling of microelectronic devices is presented. Works on single-fan and multi-fan for fluidic studies provides the background information for the present study. Next, the experimental studies on heat transfer analysis of single-fan and multi-fan are outlined, followed by detailed review of numerical fluid flow and heat transfer studies. Subsequently, a survey of the published works on the optimization and application of the piezofan is carried out, before concluding with the general remarks.

2.1 Cooling of Microelectronic Devices

Advances in the field of electronics have resulted in a significant increase in density integration, clock rates, and miniaturization of modern electronics. This resulted in dissipation of high heat flux, which linearly relates to the temperature at the chip level and creates thermal failures such as mechanical stresses, thermal debonding and thermal fracture. Managing temperature and its negative effects on electronic packages need to be considered, to ensure optimal performance and reliability (Bailey, 2008; Mochizuki et al., 2008).

Natural convection cooling is obviously advantageous for low power dissipating devices since it offers low-cost, energy-free, and noise-free operation

(Tou et al., 1999; Adams et al., 1999). An additional means of passive cooling namely finned heat sink has been adapted (Ledezma and Bejan, 1995) since it provides a large surface area for the dissipation of heat and effectively reduces the thermal resistance (Ismail et al., 2008). Nevertheless, the rising demand for high performance and multi functionality in electronic devices poses thermal challenges that may not be tackled by passive cooling techniques; this situation calls for active cooling techniques (Arularasan and Velraj, 2008). The cooling technology most widely used in electronics cooling was air-cooling. This is a mature technology with the least operation and maintenance cost. Rotational fans or blowers were often used to increase the bulk fluid motion. Fans are capable of supplying ample volume flow rates, but they are hindered by long-term reliability. Besides fan based cooling system reach saturation beyond a certain cooling capability, due to the development of thermal boundary layers at a certain volume flow rates (Dey and Chakraborty, 2009).

However, the true choice of the cooling solution was dependent on factors such as heat flux, power consumption, space, weight, reliability, mobility, integration, maintenance, noise level and cost (Anandan and Ramalingam, 2008; Lasance, 1995; Sauciuc et al., 2005 and Garimella, 2006). The technology that can deliver the required thermal performance with the least operation and maintenance cost becomes the winner. Table 2.1 summarizes a variety of novel alternative thermal solutions for electronics cooling with their relative advantages and disadvantages.

Table 2.1 Thermal solutions for electronics cooling

| Authors | Type | Advantages | Disadvantages |
|---|-----------------------------|--|--|
| Drost and Friedrich (1997); Hu and Chao (2008) | Absorption heat pump | <ul style="list-style-type: none"> • Low input power | <ul style="list-style-type: none"> • Sensitive to gravity • Chemical fluid |
| Bintoro et al. (2005); Chang et al. (2007) | Impinging jet | <ul style="list-style-type: none"> • High heat transfer rate | <ul style="list-style-type: none"> • Require cleaning and dehumidification • Difficult integrate at chip level |
| Harmand et al. (2011); Putra et al. (2011) | Heat pipe | <ul style="list-style-type: none"> • Lowest thermal resistant • Reliable • Cost effective | <ul style="list-style-type: none"> • Capillary pressure limit • Low surface area of contact |
| Khaled and Vafai (2011); Chiu et al. (2011) | Micro channel | <ul style="list-style-type: none"> • High heat flux | <ul style="list-style-type: none"> • Complicated • Expensive |
| Zhang et al. (2010); Huang et al. (2010) | Thermoelectric micro cooler | <ul style="list-style-type: none"> • No moving parts • Regenerating power | <ul style="list-style-type: none"> • High heat flux densities • Low coefficient (COP) |
| Filippeschi (2011); Khodabandeh and Furberg (2010) | Thermosyphon | <ul style="list-style-type: none"> • Flexibilities scale | <ul style="list-style-type: none"> • Low heat flux • Single-phase convection |
| Wu and Du (2011); Ribeiro et al. (2010) | Vapor compression | <ul style="list-style-type: none"> • High heat flux | <ul style="list-style-type: none"> • Expensive • Noisy • High input power |
| Kim et al. (2008a); Kim et al. (2008b) | Vapor absorption | <ul style="list-style-type: none"> • High heat flux | <ul style="list-style-type: none"> • Chemical fluid • Bulky size |
| Wong et al. (2011); Li and Chiang (2011) | Vapor chamber | <ul style="list-style-type: none"> • Lowest thermal resistant • Reliable • Cost effective | <ul style="list-style-type: none"> • Lack of flexibility • Need connector • Large volume |

Based on the works of Sauciuc (2006) and Mochizuki et al. (2011), piezofan was one of the best techniques that could cope up with those aforementioned factors. It was particularly attractive due to their operational simplicity, no noise, small size and low power consumption. Piezofan comprise a thin flexible blade attached to a piezoelectric patch actuated at its resonant frequency by a periodically alternating electric voltage. The vibrating of the blade at resonate frequency under the actuating voltage, generated an optimal airflow with low power consumption. As a result, a significant improvement in the heat transfer performance was obtained.

2.2 Experiments on Piezofan in Fluidic Studies

2.2.1 Single-fan Oscillation

Toda (1979) conducted experiments using piezofan, constructed as a multilayered PVF₂ bimorph cantilever. They presented simplified models for airflow and vibration. The observed resonance frequency was larger than the value predicted from theory, and this difference increased as shorter fans were considered. However, their results showed good agreement with theory for airflow from longer fans (lower frequencies).

Yorinaga et al. (1985) introduced a new type of a piezofan that could supply sufficient and constant airflow without any structural destruction for a long time since the flexible blade resonated in large amplitude, and the bimorph vibrated with very small amplitude. They designed a modified bimorph based on the theory of a dynamic absorber and succeeded to obtain stable vibration and sufficient airflow. Yoo et al. (1994) fabricated various kinds of piezofans for application to a component cooling apparatus. The piezoelectric ceramic substrates were

manufactured by using a PZT-5 raw materials. They concluded that, the resonance frequency of the vibrating plate decreased with the increasing plate length under a constant piezoelectric ceramic length, wind velocity increased with the increasing applied voltage and displacement appeared large in case of phosphor copper with excellent elastic properties.

Yoo et al. (2000) developed and investigated many types of piezofans. Fans were constructed using bronze, brass, aluminum with PZT patches and had lengths from 32 to 35 mm. All fans operated at 60 Hz and at two voltage levels, 110 and 220 VAC, which produced different vibration amplitudes and airflow rates. The measured air velocity was found to be highly dependent on the maximum tip velocity. They also found that the most effective fan was made from a phosphor bronze shim and with PZT in a bimorph configuration whose width was equal to that of the piezoelectric patch.

Acikalin and co-workers (2003) conducted flow visualization experiments to gain insight on the flow induced by piezofans. The piezofan with 60 Hz actuation was located at the center of the domain and sandwiched between a black bottom surface, transparent acrylic top sheet, with the side walls were kept sufficiently away from the fan to reduce interference effects on the flow field. A baffle was placed along the axis of the fan spanning the full length of the setup. A laser sheet illuminated the field from the side, parallel to the top Plexiglas surface, and smoke was seeded from a theatrical fog generator. A digital video camera was placed above the setup to capture the scattered light from the smoke particles in the domain. This work was extended by Acikalin et al., (2004) for additional visualization

experiments. A piezofan actuated at 20Hz was placed inside a clear acrylic enclosure. Both observations found that suction occurred near the clamp and near the tip of the piezofan and two circulation zones having opposite directions were generated on each side.

Kim et al. (2004) investigated the flow field created by a vibrating plate using phase-resolved particle image velocimetry (PIV) and smoke visualization techniques. The actuated cantilever was 31 mm long and vibrated at 180 Hz with tip displacements ranging from 0.74 to 1.4 mm. Counter-rotating vortices were shed each time the blade passed the original position i.e. at twice the vibration frequency. Between these two vortices and just beyond the tip, a region was formed where the maximum fluid velocity occurred, and was found to be roughly four times that of the maximum tip velocity. They also found that the flow field was two-dimensional near the cantilever tip and became more complex and three-dimensional further downstream.

Wait et al. (2007) experimented piezofan at the higher resonance modes by varying its length. Detailed flow visualizations were performed to understand both the transient and steady state fluid motion around the piezofan. The setup was quite similar to that of Acikalin et al. (2003). They observed that the flow patterns at different resonance modes changed according to the deformation mode shape of the piezofan. Areas of recirculation were created between two nodes of the piezofan and vortices were shed from the tip. The bulk fluid motion decreased as the mode number increased due to the decrease in amplitude. Additionally, as the motion of the piezofan became more complex along the length of the blade, different portions of

the fan blade moving in opposing directions tend to counteract, rather than augmenting the flow. It was also observed that decreasing the length of the fan decreased the flow volume due to smaller amplitude of vibration, and lesser surface area available to “push” the fluid.

Acikalin and Garimella (2009) conducted flow visualization and PIV experiments in a liquid at an amplitude of 1.5 mm (peak-peak) at two different gaps. The dielectric liquid was used for submersion of the whole setup, including the piezofan. A piezofan was sandwiched between two transparent acrylic plates, clamped by a copper block and positioned at the center of the setup. A light sheet generated from a diode-pumped Nd:YVO₄ laser using a cylindrical aspheric lens with a hyperbolic profile illuminated the mid-plane of the experimental setup. A high-speed camera captured top-view images of the flow field. Flour particles were used as tracers to visualize the flow patterns. For both the gaps, the shapes of the streamlines were very similar for the regions close to the piezofan but not near the piezofan tip. Two separation flows were observed; fluid approached the fan and fluid entered the domain and ejected from the heater surface. Eastman and Kimber (2009) analyzed the flow field of a piezofan in a glass enclosure using PIV for a range of Reynolds numbers. It was found that larger Reynolds number gave a more repeatable and predictable vortex path. It was also observed that lower amplitudes tend to give a stronger flow in the x-direction as well as having a higher overall flow velocity in a 2-D view.

Kim et al. (2011) investigated the velocity field around a vibrating cantilever plate using phase-locked PIV. Experiments were performed at three different

Reynolds numbers based on the tip amplitude and frequency of the cantilever. The averaged vector fields showed that a pseudo-jet flow was dominated by vortical structures.

2.2.2 Multi-fan Oscillation

Majority of previous studies have considered single-fan. However, the studies on multi-fan are still lacking. It is practically important to configure multi-fan, and the complexity increases substantially in describing the structural, fluidic, and heat transfer behavior.

Ihara and Watanabe (1994) investigated flow field generated from single and two flexible cantilevers for in-phase and out-of-phase vibration at three different pitches. These cantilevers were sandwiched between two parallel plates to approximate a two-dimensional flow field as shown in Figure 2.1. The smoke wire method was employed for flow visualization. Comparisons of flow field and volumetric flow rate have been made. The volumetric flow rate for in-phase vibration of two cantilevers was found to be approximately double that of a single cantilever.

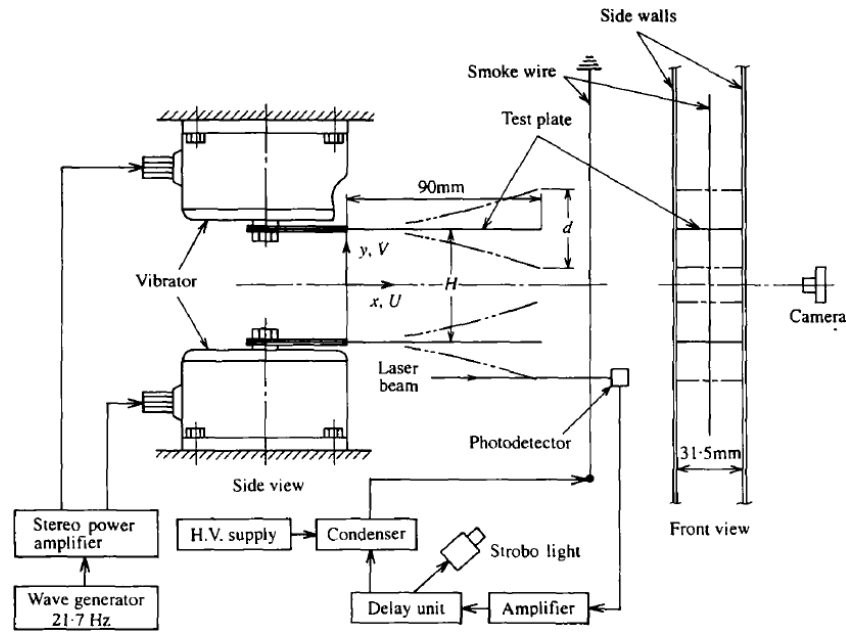


Figure 2.1 Side and front views of oscillating plates and experimental arrangement (Ihara and Watanabe, 1994)

Schmidt (1994) performed mass transfer measurements on a vertical surface mounted near two piezofans. The fan pitch was kept constant and vibrated out of phase. Power-law correlations were found to reasonably describe both maximum and surface-averaged Sherwood numbers for three different distances from the vertical surface. The contours of Sherwood numbers formed symmetrically about the midpoint of fan separation in each case. Obviously, changes in fan vibration parameters influenced the flow field and heat transfer performance. A number of studies have shown that the presence of a second oscillating blade could alter the vibration characteristics of a vibrating cantilever.

Linderman et al. (2005) analyzed flow rates produced by single and linear array of vibrating blades in a channel. It has been observed that the flow rate for the single cantilever varied linearly with frequency, length, and vibration amplitude and the flow rate was nearly tripled whenever three fans were placed in series. However,

the fan's pitch variable was neglected and the interaction between neighboring fans was not captured. Kimber et al. (2006) measured resonance frequency and quality factors for fans vibrating in air and observed a decrease in viscous drag when the fans vibrated in phase. Larger vibration amplitudes of the fans were found for a given input signal relative to a single-fan.

Kimber et al. (2007) presented experiments on multi-fan in air and within a vacuum chamber to isolate the source of coupling. Two piezofans were mounted in a vacuum chamber and excited in-phase at a frequency of 60 Hz at four discrete amplitudes and two fan pitches. Optical viewport provided the capability to capture vibration signals. The result showed that the amplitudes were nearly double regardless of whether a single-fan or two fans considered. In contrast, the vibration amplitude for two fans under atmospheric conditions was found larger compared to that of the single-fan.

Kimber et al. (2008) studied the effect of pressure and flow rate generated from vibrating cantilevers. Design tools similar to the often-used fan laws were proposed in order to predict the pressure and flow rate. The effect of proximity of surrounding walls to the piezofan was also studied by using three enclosures of different sizes. It was found that the performance was highly dependent on both the vibration amplitude and frequency. They also developed predictive relationships to describe the experimental trends, provided insight into the sensitivities of pressure and flow rate to these operating parameters. The tip velocity contributed nearly quadratic dependence on flow rate, while the vibration frequency extremely influenced the determination of pressure. It was also found that a large enclosure had

relatively little influence on the pressure or flow rate; as the size of the enclosure became smaller, only pressure was adversely affected and the inlet flow was found to be freely open for experiencing the largest amplitude to ensure the largest flow rate possible. Kimber et al. (2009a) performed further investigation, for the aforementioned effect. Direct comparison was made between two commercial axial fans, in terms of overall performance, and the efficiency with which energy was imparted to the fluid. It was observed that piezofans were nearly 10 times more efficient in converting the input power to useful energy imparted to the fluid.

Kimber et al. (2009b) experimentally quantified the fluid loading (added mass and damping) on arrays of cantilevers vibrating face-to-face and edge-to-edge. Two sets of experiments were conducted; in air and vacuum. The effect of air resonance frequency and flow rate for a range of pitches and input voltages were determined. They observed a substantial decrease in the fluid damping with in-phase vibration, while the converse was true with out-of-phase vibration for the face-to-face orientation. The edge-to-edge, out-of-phase vibration exhibited a decrease in fluid damping, and in-phase vibration caused an increase.

2.3 Experiments on Piezofan in Heat Transfer

2.3.1 Single-fan Configuration

Toda (1981) was the first to study piezofan exclusively on heat transfer enhancement, on a heated surface. The piezofan vibrated at 13 Hz with maximum airflow velocity of 1.4 m/s, caused 17°C decrease in temperature on the power transistor panel of a TV receiver. In addition, the temperature inside the receiver was also reduced by 5°C.

Kimber et al. (2007) measured the local heat transfer characteristics of piezofans by using infrared camera. The experimental setup included a film plate, coated on both sides with a thin layer of Krylon #1602 black paint with constant heat flux surface, mounted in a vertical position on an optical table. A piezofan was mounted normal to the heat source, with one side linearly adjustable, while a laser displacement sensor captured the vibration signal of the fan tip. A plexiglass enclosure was built around the entire setup to isolate it from extraneous flows within the room. Four vibration amplitudes with certain distance gaps and amplitude was considered. They found that the thermal map of the local heat transfer coefficient transitioned from a lobed shape at small gaps to an almost circular shape at intermediate gaps and became elliptical in shape at larger gaps. In addition, the value of optimum gap was dependent on the vibration amplitude. They proposed a predictive correlation for stagnation-region and area-averaged local Nusselt numbers.

Liu et al. (2009) investigated the thermal performance of piezofans with various blade geometries. They also considered the influence of geometric parameters such as the horizontal/vertical arrangement, and location of the piezofan. Experiments were carried out in an environmental chamber with room temperature at 25°C. It consisted of an aluminum plate attached on Kapton heater with an identical size as the test plate with the power inputs ranging from 3-15 W by a DC power supply, and an insulation box. The heat transfer performance for vertical arrangement showed a symmetrical distribution and peaked at the center region whereas the horizontal arrangement possessed an asymmetrical distribution and showed an early peak.

2.3.2 Multi-fan Configuration

Local and average heat transfer coefficients on a vertical surface cooled by a piezofan were evaluated by Schmidt (1994) using the naphthalene sublimation technique. The piezofan blades vibrated out of phase, and the fan frequency pitch was kept constant. A rectangular hole was made at the centre of the Plexiglas sheet and three cast naphthalene plates were installed side by side in this hole during the test runs. Power law correlations were found to reasonably describe both maximum and surface-averaged Sherwood numbers for three separate distances from the vertical surface. The local Sherwood number indicated the surface locations where the fan provided the most effective cooling. The maximum coefficient occurred at the midpoint of the fan blade for all the three fan-to-surface separations.

Kimber et al. (2009c) conducted an experimental study for a pair of piezofans in horizontal and vertical orientations. The piezofans pitch and tip gap were the primary factors considered in this investigation. They found that the vibration amplitude increased dramatically for in-phase vibration in the horizontal orientation, whereas the reverse effect was observed for out-of-phase vibration. However, for vertical orientation, out-of-phase vibration produced the highest vibration amplitude. The performance was greatest when the piezofans were closest with smallest fan pitch to the heat source. Ironically, it decreased the coverage area and average heat transfer coefficient. Nevertheless, both orientations demonstrated significant increase in the thermal performance compared to the single-fan.

Kimber and Garimella (2009d) quantified the influence of each operational parameter such as vibration frequency, amplitude and geometry of the vibrating

cantilever blade and its relative impact on thermal performance. Different fans, with fundamental resonance frequencies ranging from 60 to 250 Hz, were considered. The performance of the piezofans was maximized at a particular value of the tip gap and the heat transfer rate depended only on the frequency and amplitude of oscillation. Correlations were developed based on dimensionless parameters, which successfully predicted the thermal performance.

2.4 Numerical Studies on the Movement Object in Fluid

In the numerical studies, three formulations have been used namely: Acoustic Streaming, Vortex, and Arbitrary Lagrangian Eulerian (ALE).

2.4.1 Acoustic Streaming Flow

Faraday (1831) in his study found that a streaming motion was observed when a fluid was imposed into oscillatory motion by a vibrating boundary. In another finding, he described that currents of air rise at points of maximum vibration amplitude (the antinodes), and descend at points of minimum vibration amplitude (the nodes). This observation was believable due to the non-zero time-averaged quadratic Reynolds stress terms in the momentum equation. Rayleigh and Strutt (1945) had successfully explained this phenomenon in the theoretical term by analyzing dust pattern in Kundt's tubes. Westervelt (1955), Lighthill (1978), Nyborg (1998) and others, further advanced this theory.

Circulatory motions caused by acoustic streaming have been widely studied, where the situation has been restricted to the body with circular shape (Schlichting, 1955; Raney et al., 1954; Nyborg, 1958). The theoretical solution was based on

successive approximations (perturbation methods) with two solutions; first and second order. Each of these solutions should satisfy their respective boundary conditions. However, the limitation of this approach was that it is only possible for simple cases where the boundaries are cylinders, spheres or planes.

Loh et al. (2002) has successfully carried out the application of acoustic streaming flow for the piezofan. They developed analytical model based on Nyborg's formulation using successive approximation method for the vibrating cantilever. The gap between the two plates was small (2–20 mm), and the fluid was assumed as laminar and incompressible flow. Two distinctive acoustic streaming patterns in half-wavelength of the flexural vibrations were observed, which agreed well with the theory. However, the acoustic streaming patterns agreed well with the theory but overestimated in the streaming velocity to the fact that compressible flow that occur at high frequencies was excluded in the model.

Acikalin et al. (2003) developed 2-D models to describe the acoustic streaming flow induced by an infinite and finite, baffled piezofan vibrating at 60 Hz with vibration amplitude of 0.8 mm. The method of successive approximations was first used to derive analytical closed-form solutions and no closed-form solution was developed to solve the resulting perturbation equations. The agreement between experiment and numerical simulation was seen to be quite good, although the size and location of the outer streaming nodes were slightly different from the predicted values. The discrepancies were attributed to the following factors: the assumption of 2-D flow in the model, the baffle used in the experiments were not ideal, errors in the

model related to perturbation and incompressibility assumptions and errors resulting from the numerical methods employed.

Wan and Kuznetsov (2003) studied the efficiency of acoustic streaming for enhancing heat transfer between two parallel cantilevers. A perturbation method was employed to analyze the acoustic streaming in the gap between two cantilevers; one was vibrated while the other was stationary, with heater attached onto it. The compressible Navier–Stokes equations were decomposed into the first-order acoustic and second order streaming equations with steady state energy equation associated. These equations were discretized by the finite-difference method on a uniform mesh. Cooling effect due to acoustic streaming was observed, and it was suggested to utilize higher (ultrasonic) vibration frequency or vibration amplitude in conjunction with a heat sink for cooling of computer chips in future.

Wan et al. (2005) investigated forced convection in a narrow channel by a vibrating piezofan. The Navier-Stokes equations were decomposed into the acoustic equations and the streaming equations by the perturbation method. All governing equations were discretized by finite volume method (FVM) and Gauss-Seidel iteration method. In addition, the SIMPLER method was utilized in solving the acoustic streaming Equations. The flow field showed the combination of symmetric and counter-rotational eddies, which occupied the whole channel width, and was in agreement with the experimental results.

2.4.2 Discrete Vortex Method (DVM)

Other approaches were necessary for analysis in case large-amplitude of oscillations were employed which makes the acoustic streaming flow assumptions no longer appropriate. One of the solutions available was discrete vortex method. The discrete vortex method, which is based on the Lagrangian approach, was a grid-free method, and does not have any numerical diffusion due to the presence of the grid. This method was for the first time described by the Belotserkovsky and Lifanov (1993). A few examples of this method were: studies on separated flow (Stansby, 1985), flow analysis around a Savonius rotor (Ogawa, 1984), and flow-analysis around an inclined flat plate in a uniform flow (Kiya and Arie, 1977a, b).

Ihara and Watanabe (1994) successfully implemented this method to investigate flows around the ends of oscillating piezofans. The discrete vortex method combined with the singularity method was employed in their simulations. Three different cases were investigated: single-plate oscillation, two-plate counter-phase oscillation, and two-plate in-phase oscillation. It was observed that two vortices being formed downstream of the plate tip in one cycle under single-phase oscillation. For the case of two-plate oscillation, the effect of the distances between two plates on the flow field was studied for both oscillations in-phase and in counter-phase. It was found that for counter-phase oscillation, the flow structure was very complicated and did not agree with the numerical simulation as did the flow structure obtained for the single plate oscillation and two-plate in-phase oscillation.